nature photonics

LETTERS

PUBLISHED ONLINE: 15 JANUARY 2012 | DOI: 10.1038/NPHOTON.2011.327

X-ray pump optical probe cross-correlation study of GaAs

S. M. Durbin[1]*, T. Clevenger[1], T. Graber[2] and R. Henning[2]

Ultrafast dynamics in atomic, molecular and condensed-matter systems are increasingly being studied using optical-pump, X-ray probe techniques where subpicosecond laser pulses excite the system and X-rays detect changes in absorption spectra and local atomic structure[1–3]. New opportunities are appearing as a result of improved synchrotron capabilities and the advent of X-ray free-electron lasers[4,5]. These source improvements also allow for the reverse measurement: X-ray pump followed by optical probe. We describe here how an X-ray pump beam transforms a thin GaAs specimen from a strong absorber into a nearly transparent window in less than 100 ps, for laser photon energies just above the bandgap. We find the opposite effect—X-ray induced optical opacity—for photon energies just below the bandgap. This raises interesting questions about the ultrafast many-body response of semiconductors to X-ray absorption, and provides a new approach for an X-ray/optical cross-correlator for synchrotron and X-ray free-electron laser applications.

Several experimental studies have previously reported cross-correlation effects between optical and X-ray pulses. Kraessig *et al.* made use of a change in hard X-ray absorption in krypton atoms ionized by an ultrafast infrared laser pulse[6], while Gahl *et al.* measured the change in optical reflectivity from GaAs caused by 40 eV photons from an X-ray free-electron laser (XFEL)[7]. We are also interested in semiconducting GaAs, and in particular how the X-ray photo-absorption process stimulates a range of many-body responses that can be probed by optical transmission at the bandgap. From these synchrotron-based X-ray pump/optical probe studies, we report three unique experimental observations: X-ray-induced optical transparency, X-ray-induced optical opacity and the evolution from non-equilibrium electronic excitations to an equilibrium temperature response over the range 1×10^{-11} to 1×10^{-4} s.

First, it is useful to consider how X-rays create valence and conduction band excitations in a semiconductor. When X-ray absorption leads to electron ejection from an atomic core level, the photoelectron traverses dozens of unit cells while inelastically scattering hundreds or thousands of valence electrons high into the conduction band[8]. These hot electrons thermalize by electron–electron and electron–plasmon scattering, and settle into the lowest states of the conduction band while interacting with lattice phonons, a process extending into picoseconds and longer[9]. The deep core hole left behind is filled by a higher-level core electron, sometimes accompanied by fluorescence, but for lighter elements the emission of an Auger electron is more likely. This replaces a deep core hole with two higher ones, and the Auger electron inelastically scatters many more carriers to the conduction and valence bands. This is repeated with higher core levels, creating multiple localized holes that eventually cascade up to become mobile valence band holes[10].

In our experiments an ~60-μm-thick GaAs specimen absorbs an intense, 80 ps full-width at half-maximum (FWHM) synchrotron X-ray pump pulse. The transmission of a monochromatic 3 ps (FWHM) laser probe pulse near the bandgap energy was then measured as a function of the pump–probe delay time. The transmitted intensity versus time delay for $\lambda = 860$ nm, normalized to the signal without X-rays, is shown in Fig. 1. Also shown is the time profile of the X-ray pulse (convoluted with laser jitter) and the time-integrated fluence, which matches the initial data quite well. The specimen switched from optically opaque to transparent within the duration of the X-ray pulse. An 860 nm photon has just enough energy (1.44 eV) to excite a valence electron across the direct bandgap into the conduction band (~1.43 eV). The induced transparency decays with a time constant of 1.1 ns (Fig. 1, inset). Transparency was observed from ~880 to 840 nm, a bandwidth of ~70 meV. The 40-fold increase in transmitted signal

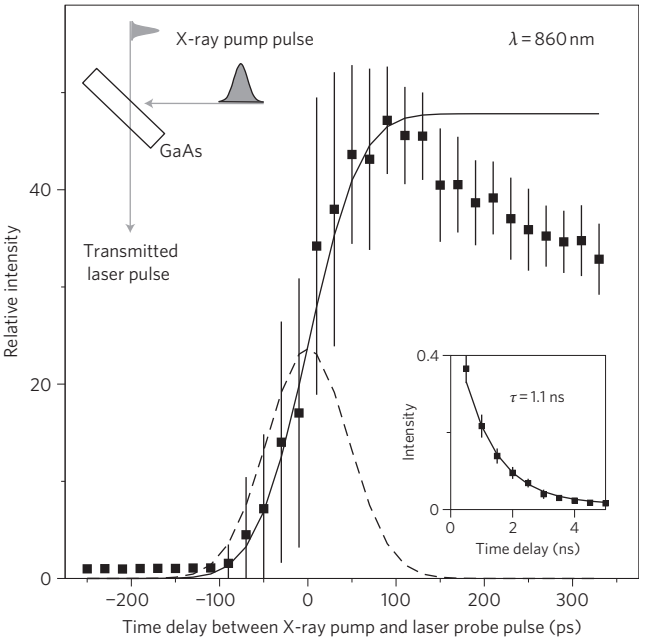

Figure 1 | Transmission at 860 nm versus time after X-ray pump pulse. Data points are normalized to the transmitted intensity before X-ray excitation and are the average of 100 shots. Error bars are the standard deviation of 100 shots and are largely due to laser/X-ray pulse timing jitter. Dashed curve: Gaussian time profile of X-ray pulses. Solid curve: integral, which matches data at the transition region. Inset (top): scattering geometry, with GaAs surface at the intersection of the X-ray and laser beams. Inset (bottom): transmission at longer times, fit to an exponential decay with a lifetime of 1.1 ns.

[1]Department of Physics, Purdue University, West Lafayette, Indiana 47907, USA, [2]The Center for Advanced Radiation Sources, University of Chicago, Chicago, Illinois 60637, USA. *e-mail: durbin@purdue.edu

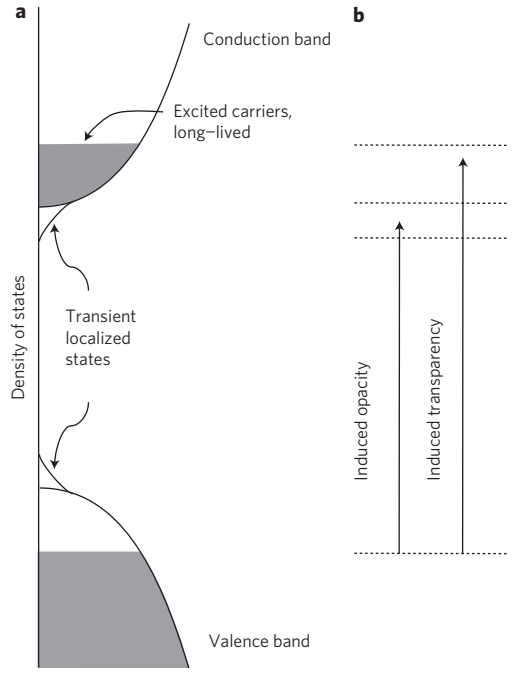

Figure 2 | Model for X-ray-induced transmission and absorption. a, Ideal semiconductor density of states, with a filled valence band separated from an empty conduction band by energy gap E_g. Photons with energy less than E_g are transmitted, and are absorbed by promoting an electron from the valence to the conduction band if the energy exceeds E_g. **b**, Intense X-ray excitation fills the states at the bottom of the conduction band, blocking absorption of photons with energies just above the bandgap energy. Induced absorption for photons with energy just below the bandgap could arise from transient localized states at the band edges, as seen with doped semiconductors.

suggests that this could be a useful X-ray/optical cross-correlator for high-intensity synchrotron and XFEL beams.

A simplified model for describing this result is shown in Fig. 2. Before X-rays arrive, the ideal semiconductor density of states at the direct bandgap is assumed to have a fully occupied valence band and an empty conduction band. The inelastic scattering of energetic photoelectrons and Auger electrons creates a high density of carriers, which fill the lowest energy levels in these bands. Originally, a photon with energy just above E_{gap} would be strongly absorbed by promoting an electron across the gap. Now, however, the top valence states are empty and the bottom conduction band states are occupied, blocking photon absorption at this energy. This persists until electron–hole recombination fills the valence band again (lifetime, ~1.1 ns). (A similar optically induced shift in the bandgap is sometimes referred to as the Burstein–Moss effect[11,12].)

The large induced transparency response could make thin GaAs a useful cross-correlator for determining X-ray pump/optical probe arrival times. By using white pulses instead of monochromatic light, the entire spectrum could be measured in a single shot, and standard chirping techniques could provide additional sensitivity. This could be especially useful for femtosecond XFEL sources, where it is desirable to directly measure X-ray pulse jitter at the experimental station instead of relying on measurements of upstream particle bunches.

The time-dependent absorption factors ($\mu x = -\ln(T)$, where T is the transmitted fraction) are shown in Fig. 3 for laser wavelengths spanning the bandgap (850–900 nm). The large X-ray-induced transparency is gradually replaced by induced absorption at 900 nm; that is, X-ray-induced opacity occurs for photon energies just below the bandgap. Absorption nearly doubles at 900 nm, where the specimen would otherwise be transparent, indicating that X-rays have somehow created a new mechanism for optical absorption below the conduction band edge. This induced optical opacity approximately follows the X-ray pulse time profile, whereas the induced optical transparency largely follows the integrated fluence (Fig. 1). The latter is expected, because the carrier recombination lifetime (1.1 ns) is much longer than the X-ray pulse. States responsible for opacity must have much shorter lifetimes, which excludes any absorption mechanism that directly depends on the excited carriers.

In considering how X-ray-induced optical absorption arises, it is important to remember a crucial difference between these measurements and ultrafast laser studies of GaAs: intense X-ray pulses produce a large number of localized core holes that are absent when pumping with optical lasers. The density of X-ray absorption sites created by each X-ray pump pulse is $\sim 0.5 \times 10^{17}$ cm^{-3}. A localized core hole has a Coulomb potential like that of an ionized donor atom. In transport studies, doping levels of $\sim 1 \times 10^{17}$ cm^{-3} and above have caused observable bandgap narrowing due to induced band tail states[13,14]. The 1×10^{17} cm^{-3} absorption site density, however, must be corrected for the core hole lifetime relative to the 100 ps pulse duration to obtain the instantaneous density. A K-shell hole with a 1×10^{-15} s lifetime would yield an effective dopant density of only 1×10^{12} cm^{-3}; the multiple shallower holes from subsequent Auger processes may increase this by another order of magnitude. These effective dopant densities seem small, but the lower detectable limit in optical measurements (as opposed to transport studies) is not clear[15]. On the other hand, these localized core holes ultimately convert into delocalized valence band holes, but their long lifetimes (1×10^{-9} s) preclude them from causing the induced absorption. Given the high density of X-ray absorption sites and the range of lifetimes experienced by the subsequent core holes, we suggest that theoretical treatments of bandgap changes in highly excited GaAs be expanded to

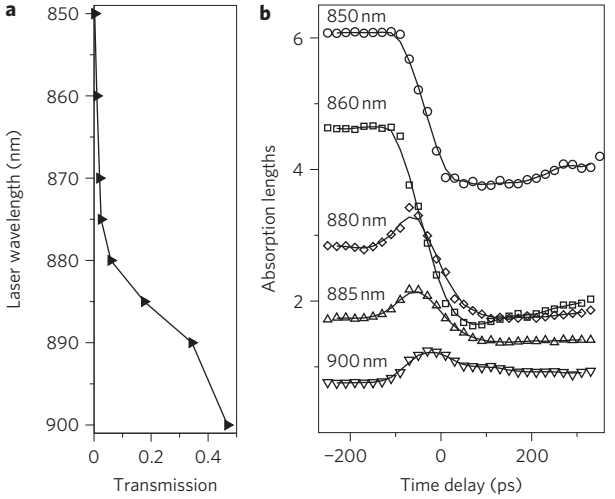

Figure 3 | Absorption factor ($\mu(\lambda)L = -\ln(T)$) versus time delay. $\mu(\lambda)L$ is the product of the absorption coefficient and the thickness, and the transmitted fraction is described by $T = (1 - R)\exp(-\mu x)$. Reflectivity R is calculated from the Fresnel relations and the GaAs dielectric constants. Any time dependence of R is assumed to be small and has been omitted. **a**, Laser beam transmitted fraction T (without X-rays) versus wavelength from below-gap (900 nm) to above-gap (850 nm) values. **b**, Exponential factor $\mu(\lambda)L$ for the GaAs specimen versus time delay for wavelengths of 850–900 nm. Note that the absorption factor profile approximates the Gaussian profile of the X-ray pulses for sub-gap wavelengths, consistent with the short-lived states induced by the X-rays (see text).

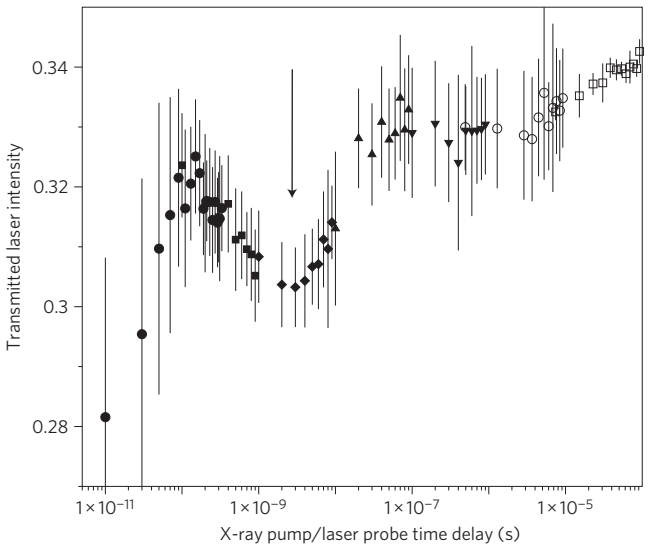

Figure 4 | Transmission at 890 nm from 1×10^{-11} to 1×10^{-4} s. Induced opacity is seen as the dip below 1×10^{-10} s. The arrow denotes the second opacity region at $\sim 1 \times 10^{-9}$ s. The gradual increase at longer times reflects the increase in bandgap as the specimen cools. Different symbols refer to separate scans of overlapping time domains. Error bars are standard deviation of measurements from 100 X-ray pulses, except the last set (square symbols) of smaller error bars, which are calculated from multiple repeated scans.

include the localized core holes, to better understand the origins of X-ray induced optical absorption.

Because excited electrons can be a source of phonons as they thermalize, the possibility of absorption assisted by longitudinal optical (LO) phonons must be considered. Several ultrafast laser pump–probe transmission studies of GaAs have been carried out near the bandgap[16–19], but none reports evidence for phonon-assisted absorption, even for pair densities in the 1×10^{18} to 1×10^{19} cm^{-3} range (the pair density in our measurements is estimated to be $\sim 0.5 \times 10^{20}$ cm^{-3}; see Methods). Recent theoretical studies of optical refrigeration in GaAs have considered the possibility of phonon-assisted absorption. However, there is only limited comparison with experiment[20–22]. Furthermore, experiment and theory[15,21,23] agree that increasing electron–hole pair densities cause a decrease in any LO-phonon assisted absorption, because the plasma effectively screens the transient dipole moments from the LO phonons. With densities near 1×10^{20} cm^{-3}, this suggests that phonon-assisted absorption should be greatly suppressed in the X-ray-pumped results.

Finally, we show (Fig. 4) sub-bandgap transmission (at 890 nm) for time delays from 1×10^{-11} s to 1×10^{-4} s. The induced opacity that tracks the X-ray pulse is seen as the dip below 100 ps. The drift upwards after $\sim 1 \times 10^{-7}$ s is consistent with an elevated temperature gradually cooling to room temperature, because the bandgap in GaAs narrows with increased temperature[24,25] By assigning the drop in transmission to a shift in the bandgap, we can use the published temperature dependence of the GaAs bandgap to equate this to a temperature increase of ~ 4 K at 1×10^{-7} s.

For times less than 1×10^{-8} s, however, it appears that non-equilibrium processes dominate the optical transmission. A second dip in transmission (that is, increased opacity) is seen at $\sim 1 \times 10^{-9}$ s. There is clearly a competition among mechanisms responsible for this complex behaviour, for example, induced band tail states, electron–hole recombination, free-carrier scattering, non-equilibrium phonon excitations, and so on. Recent work on InP and InSb have also shown non-equilibrium phonon distributions for nanoseconds after laser excitation[26]. We see here that X-ray pumping causes the system to remain out of equilibrium for even longer times. Comparing these data with future X-ray pump/optical probe transmission measurements on an indirect-gap semiconductor (such as germanium) could help separate phonon and electron contributions.

In conclusion, we have demonstrated that intense X-ray illumination of GaAs generates ultrafast many-body responses at the semiconductor bandgap that are readily probed with optical pulses. The X-ray excitations can induce optical transparency above the gap and optical absorption just below the gap, using intense 80 ps pulses from an X-ray synchrotron. Additional non-equilibrium phenomena are evident at gap energies for many nanoseconds after excitation. The extension of these measurements with femtosecond XFEL pulses would provide greater insight into the ultrafast many-body response of semiconductors to X-ray excitation.

Methods

Measurements were conducted at the Advanced Photon Source X-ray synchrotron facility, using the combined output of two undulator insertion devices at the BioCARS Sector 14 end station[27]. Their full spectral output, peaking at 12 keV with 4% bandwidth and focused to $\sim 40 \times 100$ μm^2, is composed of pulses of 80 ps FWHM duration at 6.5 MHz. With a stored current of 100 mA, the energy deposited at the sample was 21 μJ/pulse, corresponding to $\sim 1 \times 10^{10}$ X-rays per pulse or nearly 1,000 times larger than with standard monochromated beams. A high-speed chopper was used to isolate individual pulses at 4 Hz (typically). X-ray pulses were synchronized with laser pulses from an optical parametric amplifier system, producing 1.2 ps (root-mean square, r.m.s.) pulses over the wavelength range 850–900 nm with 6 nm FWHM bandwidth. The power per pulse was 0.07 μJ into a 50 μm spot size, and the jitter in time delay between X-ray and laser pulses was $\sigma = 32$ ps r.m.s. The time delay between X-ray and optical pulses was measured with fast photodiodes and a high-bandwidth digital oscilloscope with 3.6 ps (r.m.s.) resolution. Convolution of the X-ray pulse with this jitter yields a Gaussian with 110 ps FWHM.

Samples were cut from a 350 μm semi-insulating GaAs wafer and mounted on sapphire substrates using a thin crystal bond adhesive, then ground with SiC grit and diamond paste until the thickness was ~ 60 μm. The GaAs/sapphire specimens were positioned with the ground surface at the intersection of the perpendicular X-ray and laser beams, usually at 45° to each (Fig. 1). X-ray absorption lengths at the energies used were ~ 30 μm, so most of the incident X-rays were absorbed in the GaAs[28]. Assuming the X-rays were absorbed throughout the 60 μm specimen thickness, the density of absorption sites was $\sim 0.5 \times 10^{17}$ cm^{-3}. Furthermore, if all of the X-ray energy was ultimately converted to electron–hole pairs at ~ 10 eV/pair[8], the cumulative pair density after one pulse was $\sim 0.5 \times 10^{20}$ cm^{-3}.

Received 14 June 2011; accepted 28 November 2011; published online 15 January 2012

References

1. Bostedt, C. *et al.* Experiments at FLASH. *Nuclear Instruments & Methods in Physics Research Section A—Accelerators Spectrometers Detectors and Associated Equipment* **601,** 108–122 (2009).
2. Glownia, J. M. *et al.* Time-resolved pump–probe experiments at the LCLS. *Opt. Express* **18,** 17620–17630 (2010).
3. Bressler, C. & Chergui, M. Molecular structural dynamics probed by ultrafast X-ray absorption spectroscopy. *Annu. Rev. Phys. Chem.* **61,** 263–282 (2010).
4. McNeil, B. W. J. & Thompson, N. R. X-ray free-electron lasers. *Nature Photon.* **4,** 814–821 (2010).
5. Emma, P. *et al.* First lasing and operation of an angstrom-wavelength free-electron laser. *Nature Photon.* **4,** 641–647 (2010).
6. Kraessig, B. *et al.* A simple cross-correlation technique between infrared and hard X-ray pulses. *Appl. Phys. Lett.* **94,** 171113 (2009).
7. Gahl, C. *et al.* A femtosecond X-ray/optical cross-correlator. *Nature Photon.* **2,** 165–169 (2008).
8. Ziaja, B., London, R. A. & Hajdu, J. Ionization by impact electrons in solids: electron mean free path fitted over a wide energy range. *J. Appl. Phys.* **99,** 033514 (2006).
9. Schafer, W. & Wegener, M. *Semiconductor Optics and Transport Phenomena*, Advanced Texts in Physics (Springer, 2002).
10. Mcguire, E. J. Atomic L-shell Coster–Kronig, Auger, and radiative rates and fluorescence yields for Na-Th. *Phys. Rev. A* **3,** 587–594 (1971).
11. Moss, T. S. The interpretation of the properties of indium antimonide. *Proc. Phys. Soc. London B* **67,** 775–782 (1954).
12. Burstein, E. Anomalous optical absorption limit in InSb. *Phys. Rev.* **93,** 632–633 (1954).

13. Van Mieghem, P. Theory of band tails in heavily doped semiconductors. *Rev. Mod. Phys.* **64,** 755–793 (1992).
14. Sze, S. M. & Ng, K. K. *Physics of Semiconductor Devices* 3rd edn (Wiley-Interscience, 2007).
15. Liebler, J. & Haug, H. Theory of the band-tail absorption saturation in polar semiconductors. *Phys. Rev. B* **41,** 5843–5856 (1990).
16. Oudar, J. L., Hulin, D., Migus, A., Antonetti, A. & Alexandre, F. Subpicosecond spectral hole burning due to non-thermalized photoexcited carriers in gaas. *Phys. Rev. Lett.* **55,** 2074–2077 (1985).
17. Schoenlein, R. W., Lin, W. Z., Ippen, E. P. & Fujimoto, J. G. Femtosecond hot-carrier energy relaxation in GaAs. *Appl. Phys. Lett.* **51,** 1442–1444 (1987).
18. Nunnenkamp, J., Collet, J. H., Klebniczki, J., Kuhl, J. & Ploog, K. Subpicosecond kinetics of band-edge absorption in $Al_{0.25}Ga_{0.75}As$. *Phys. Rev. B* **43,** 14047–14054 (1991).
19. Chang, Y. M. & Chang, N. A. Coherent longitudinal optical phonon and plasmon coupling in GaAs. *Appl. Phys. Lett.* **81,** 3771–3773 (2002).
20. Rupper, G., Kwong, N. H. & Binder, R. Large excitonic enhancement of optical refrigeration in semiconductors. *Phys. Rev. Lett.* **97,** 117401 (2006).
21. Khurgin, J. B. Role of bandtail states in laser cooling of semiconductors. *Phys. Rev. B* **77,** 235206 (2008).
22. Sturge, M. D. Optical absorption of gallium arsenide between 0.6 and 2.75 eV. *Phys. Rev.* **127,** 768–773 (1962).
23. Banyai, L. & Koch, S. W. A simple theory for the effects of plasma screening on the optical-spectra of highly excited semiconductors. *Zeitschrift Fur Physik B* **63,** 283–291 (1986).
24. Grilli, E., Guzzi, M., Zamboni, R. & Pavesi, L. High-precision determination of the temperature-dependence of the fundamental energy-gap in gallium-arsenide. *Phys. Rev. B* **45,** 1638–1644 (1992).
25. Passler, R. Dispersion-related description of temperature dependencies of band gaps in semiconductors. *Phys. Rev. B* **66,** 085201 (2002).
26. Trigo, M. *et al.* Imaging nonequilibrium atomic vibrations with X-ray diffuse scattering. *Phys. Rev. B* **82,** 235205 (2010).
27. Graber, T. *et al.* BioCARS: a synchrotron resource for time-resolved X-ray science. *J. Synch. Rad.* **18,** 658–670 (2011).
28. Henke, B. L., Gullikson, E. M. & Davis, J. C. X-ray interactions—photoabsorption, scattering, transmission, and reflection at $e = 50$–$30{,}000$ eV, $z = 1$–92. *Atomic Data and Nuclear Data Tables* **54,** 181–342 (1993).

Acknowledgements

This research was supported by the US Department of Energy, Office of Basic Energy Science (award no. DE-SC0004078). Use of the Advanced Photon Source was supported by the US Department of Energy, Basic Energy Sciences, Office of Science (contract no. DE-AC02-06CH11357). Use of the BioCARS Sector 14 was supported by the National Institutes of Health, National Center for Research Resources (grant no. RR007707). The time-resolved set-up at Sector 14 was funded in part through a collaboration with Philip Anfinrud (NIH/NIDDK).

Author contributions

All four authors were substantially involved with acquiring the data. S.M.D. analysed the results and wrote the manuscript, with assistance from T.G.

Additional information

The authors declare no competing financial interests. Reprints and permission information is available online at http://www.nature.com/reprints. Correspondence and requests for materials should be addressed to S.M.D.